Applied Mathematics & Information Sciences
An International Journal

http://dx.doi.org/10.18576/amis/100424

The Rotational Motion of the Electromagnetic Symmetric Rigid Body

T. S. Amer[*]

Department of Mathematics, Faculty of Science, Tanta University, Tanta 3127, Egypt.

Received: 6 Apr. 2016, Revised: 23 May 2016, Accepted: 24 May 2016
Published online: 1 Jul. 2016

Abstract: In the present article, the rotational motion of a symmetric rigid body (gyro) about a fixed point close to Lagrange's case is studied. This gyro is acted upon by a perturbing moment vector, a third component of a gyro moment vector, and a variable restoring moment vector. The angular velocity of the gyro is assumed to be sufficiently large, its direction is close to the axis of dynamic symmetry, and the perturbing moments are small as compared to the restoring ones. These conditions permit to introduce a small parameter. Averaged systems of the equations of motion in the first and second approximations are obtained. Also, the evolution of the precession angle up to the second approximation is determined. The graphical representations of the attained angles and its interpretations are presented.

Keywords: Euler's equations, Rigid body motion, Perturbation methods

1 Introduction

The rotational motion of a rigid body about a fixed point in a uniform force field or in a Newtonian one is one of the important problems in the theoretical classical mechanics. These problems require complicated mathematical techniques because that motion is governed by six non-linear differential equations with three first integrals [1]. The Poincaré small parameter method [2] was used to find the first terms of the series expansion of the periodic solutions of the equations of motion of a heavy rigid body about a fixed point when the body spins rapidly about the dynamical symmetry axis [3]. Some other methods are used to obtain the solutions of the rotational motion of a symmetric rigid body can be found in the works e. g. [4,5,6]. In [6], the authors studied the motion of the electromagnetic gyroscopic motion when the gyroscope moves under the influence of the uniform force field, Newtonian one, perturbed torques and restoring ones. The perturbed rotational motions of a rigid body near to Lagrange's case was investigated in [7,8,9, 10] when the restoring moment is constant and when depends on the nutation angle. Almost, the regular perturbed rotational motions of a rigid body have been studied in [11]. In [12], the author studied the same problem analogous to Lagrange top. In [13], the perturbed motions of a rotating symmetric gyrostat is studied when the gyrostatic moment is acted. The asymptotic behaviour of a Lagrange gyroscope under the influence of a weak perturbing moment for the case that closed to regular precessions is investigated in [14]. The analytical solutions of the equations of motion are obtained using the averaging method, including in [15,16,17]. The motion of a gyro having one fixed point and subject to frictional forces is studied in [18]. The frictional forces are accounted for by a model wherein the frictional torque is proportional to the angular velocity. The problem of capture and escape from resonance phenomena in rotational motions of a rigid body in a viscous medium is investigated in [19] when certain nonlinear integrable Hamiltonian systems are subjected to non-hamiltonian perturbation. In [20], the author studied the motion of a rigid body around the center of mass when it descends through the atmosphere that has a considerable effect on the behaviour of the body. The most complex problems arise when the resonance is considered. The spatial chaotic motion of a blunt body in the atmosphere when there is a periodic change in the position of the center of mass is studied in [21]. This study is considered when the body acted by a restoring moment, described by a biharmonic dependence on the spatial angle of attack, a small perturbing moment, due to the periodic change in

[*] Corresponding author e-mail: tarek.amer@science.tanta.edu.eg, tarekamer30@hotmail.com

the position of the center of mass, and a small damping moment. In [22], the uncontrolled motions of blunt-shaped spacecrafts of small elongation descended in the rarefied atmosphere are considered. The analytical formulas for the initial angular velocity of the spacecraft and for spacecraft's geometrical parameters were obtained. Works [23] and [24], are devoted to the study of perturbed motion of the rigid bodies and spacecraft, including the action of small harmonic disturbances, variability of the inertia-mass parameters, and also damping effect. In [25], the gyrostat's motion is considered in cases of unperturbed motion. In [26,27,28], the dual-spin spacecraft with variable structure was considered; also the attitude motion's evolutions were investigated with the help of full mathematical models for systems with variable structure.

In this paper, the rotational motion of a symmetric rigid body (gyro) with mass distribution near to Lagrange's case is investigated. We considered that the gyro is acted upon by the third component of the gyrostatic moment vector $\underline{\lambda}$ about the moving z axis, a variable restoring moment k which is the result of a uniform magnetic field of strength $\underline{H}$ and a point charge e that located on the symmetry axis, and a perturbing moment vector $\underline{M}$. It is assumed that the angular velocity of the gyro is very high, near to the symmetry axis, and the projections of the perturbing moment vector onto the principal axes of inertia of the body are small as compared to the restoring moment. Consequently, one can introduce a small parameter $\varepsilon << 1$. The averaging method [15,16], is used to obtain the averaged systems of the equations of motion and to evaluate the nutation and precession angles up to the first and second approximations. The graphical plots of these approximations are presented. This problem is considered as one of the important problems in mechanics. The importance of this problem is due to the wide range of its applications in various fields such as in the aero-planes, the spacecrafts, the submarines and the compasses. Moreover, the study of the rotational motion of the gyro has been motivated by industrial applications in many fields. This is because the rigid bodies provide a convenient model for the satellite-gyrostat, spacecraft and like, see [29,30,31,32].

2 Description of the problem

Consider the motion of a dynamically symmetrical rigid body (gyro) about a fixed point O, a fixed coordinate system $OXYZ$ with origin O and another rotating one $Oxyz$ fixed in the gyro and whose axes are directed along the principal axes of inertia of the gyro. This body rotates under the influence of the third component λ_3 (acted on the rotating z axis) of the gyrostatic moment vector $\underline{\lambda}$ in which the first two components are considered to be zero, perturbing moment vector $\underline{M} \equiv (M_1, M_2, M_3)$ in which $M_i (i = 1,2,3)$ represent the projections of the perturbing moment vector onto the principal inertial axes.

Let us consider the case of the gyro in which the ellipsoid of inertia is close to the ellipsoid of rotation and the center of mass of the gyro is displaced relative to center of mass O_c by an amount of order ε. Then, the principal moments of inertia and the coordinates of the center of gravity can be written in the forms [33]

$$A = A^0(1+\varepsilon\delta_1), \quad B = B^0(1+\varepsilon\delta_2), \quad A^0 \neq C, \tag{1}$$

$$x_c = \varepsilon x_1 \ell, \quad y_c = \varepsilon y_1 \ell, \quad z_c = \ell, \tag{2}$$

where A, B and C are the principal moments of inertia; δ_1 and δ_2 are dimensionless constants of order unity; A^0 is the characteristic value of moments of inertia; ε is a small parameter; x_c, y_c and z_c are the coordinates of O_c; x_1 and y_1 are dimensionless quantities that are considered finite in comparison with ε; and ℓ is the distance from O to the center of gravity.

Taking into consideration that, the gyro rotates under the action of the third component of the gyro moment vector and Lorentz force $\underline{F} = e(\underline{V} \wedge \underline{H})$ [34] in which $\underline{V} = e(\underline{\omega} \wedge \underline{\ell'})$, $\underline{\ell'} \equiv (0,0,\ell')$ where ℓ' is the distance of the position of the point charge e to O and $\underline{\omega}$ is the angular velocity vector of the gyro. So, the restoring moment of the Lorentz force has the form $\underline{M} = e(\underline{H}.\underline{\ell'})(\underline{\omega} \wedge \underline{\ell'})$.

Therefore, this moment has the components $eH\ell'^2 q\cos\theta$, $-eH\ell'^2 p\cos\theta$ and 0 in projection onto the principal axes of inertia of the gyro.

Then the equations of motion similar to Lagrange's case take the form [6,7,8,9,10]

$$\begin{cases} A\dot{p} + (C-A)qr + q\lambda_3 = mg\ell\sin\theta\cos\varphi + M_1, \\ A\dot{q} + (A-C)pr - p\lambda_3 = -mg\ell\sin\theta\sin\varphi + M_2, \\ C\dot{r} = M_3; \quad M_i = M_i(p,q,r,\psi,\theta,\varphi,t), \\ \dot{\theta} = p\cos\varphi - q\sin\varphi, \\ \dot{\varphi} = r - (p\sin\varphi + q\cos\varphi)\cot\theta, \\ \dot{\psi} = (p\sin\varphi + q\cos\varphi)\csc\theta. \end{cases} \tag{3}$$

Here, p, q and r are the components of the angular velocity vector; θ, φ and ψ are the nutation, the self-rotations and the precession angles respectively; m is the mass of the gyro; and g is the acceleration due to gravity.

So, our aim is to investigate the behavior of this system under the following assumptions [8]

$$p^2 + q^2 \ll r^2, \quad Cr^2 \gg k, \quad |M_i| \ll k \quad (i = 1,2,3). \tag{4}$$

According to these assumptions, one can introduce the small parameter ε as

$$\begin{cases} p = \varepsilon P, \quad q = \varepsilon Q, \quad k = \varepsilon K, \\ M_i = \varepsilon^2 M_i^*(P,Q,r,\psi,\theta,\varphi,t) \quad (i = 1,2,3). \end{cases} \tag{5}$$

3 The approximate solutions

In this section we will obtain the approximate solution using the averaging method [15,16]. Taking into account inequalities (4), the total restoring moment K takes the form

$$K = mg\ell + eH\ell'^2 \cos\theta \sqrt{p^2+q^2}. \tag{6}$$

Substituting (2) and (5) into system (3), one obtains directly

$$\begin{cases} A^0\dot{P} + [(C-A^0)r + (1+\varepsilon\delta_1)\lambda_3]Q = K[(1-\varepsilon\delta_1) \\ \times \sin\theta\cos\varphi - \varepsilon y_1\cos\theta] + \varepsilon[\delta_1(C-A^0) + \delta_2 A^0]Qr, \\ A^0\dot{Q} + [(A^0-C)r - (1-\varepsilon\delta_2)\lambda_3]P = -K[(1-\varepsilon\delta_2) \\ \times \sin\theta\sin\varphi - \varepsilon x_1\cos\theta] + \varepsilon[\delta_2(A^0-C) - \delta_1 A^0]Pr, \\ C\dot{r} = \varepsilon^2 K\sin\theta(y_1\sin\varphi - x_1\cos\varphi), \\ \dot{\theta} = \varepsilon(P\cos\varphi - Q\sin\varphi), \\ \dot{\varphi} = r - \varepsilon(P\sin\varphi + Q\cos\varphi)\cot\theta, \\ \dot{\psi} = \varepsilon(P\sin\varphi + Q\cos\varphi)\csc\theta. \end{cases} \tag{7}$$

The projections of the perturbing moment vector onto the principal axes of inertia can be obtained from (3)-(5) in the form

$$\begin{cases} M_1^* = -K(\delta_1\sin\theta\cos\varphi + y_1\cos\theta) \\ -[\delta_1\lambda_3 - r(\delta_1(C-A^0) + \delta_2 A^0)]Q, \\ M_2^* = K(\delta_2\sin\theta\sin\varphi + x_1\cos\theta) \\ +[\delta_2\lambda_3 + r(\delta_2(A^0-C) - \delta_1 A^0)]P, \\ M_3^* = K\sin\theta(y_1\sin\varphi - x_1\cos\varphi). \end{cases} \tag{8}$$

For $\varepsilon = 0$, the last four equations of (7) give

$$r = r_0, \quad \psi = \psi_0, \quad \theta = \theta_0, \quad \varphi = r_0 t + \varphi_0, \tag{9}$$

where r_0, ψ_0, θ_0 and φ_0 are constants, that equal to the corresponding variables at the beginning of motion.

Substituting (9) into the first two equations of system (7), the following system of second order differential equations can be obtained

$$\begin{cases} \ddot{P} + y_0^2 P = Z_0 K_0 \sin\theta_0 \sin(r_0 t + \varphi_0), \\ \ddot{Q} + y_0^2 Q = Z_0 K_0 \sin\theta_0 \cos(r_0 t + \varphi_0). \end{cases} \tag{10}$$

Integration of this system yields

$$\begin{cases} P = a\cos\gamma_0 + b\sin\gamma_0 + E_0\sin\theta_0\sin(r_0 t + \varphi_0), \\ Q = a\sin\gamma_0 - b\cos\gamma_0 + E_0\sin\theta_0\cos(r_0 t + \varphi_0), \end{cases} \tag{11}$$

where

$$\begin{cases} a = P_0 - E_0\sin\theta_0\sin\varphi_0, \quad b = -Q_0 + E_0\sin\theta_0\cos\varphi_0, \\ \gamma_0 = y_0 t, \quad y_0 = n_0 + (A^0)^{-1}\lambda_3, \\ n_0 = (C-A^0)(A^0)^{-1}r_0, \quad E_0 = z_0 k_0/(y_0^2 - r_0^2), \\ z_0 = (A^0)^{-1}(y_0 - r_0), \quad k_0 = K_0, \quad |y_0/r_0| \le 1, \quad r_0 \ne 0. \end{cases}$$

Here, P_0, Q_0 and K_0 are the initial values of the corresponding variables P, Q and K, while the variable $\gamma = \gamma_0$ has the meaning of the oscillation phase. System (7) is substantially nonlinear; therefore one can introduce an additional variable γ, defined as

$$\begin{cases} \dot{\gamma} = y, \quad \gamma(0) = 0; \quad y = n + (A^0)^{-1}\lambda_3, \\ n = (C-A^0)(A^0)^{-1}r. \end{cases} \tag{12}$$

Equations (9) and (11) determine the general solution of system (7) for $\varepsilon = 0$. According to (9), equations (11) can be rewritten in equivalent forms for P and Q, consequently one obtains

$$\begin{cases} a = P\cos\gamma + Q\sin\gamma - E\sin\theta\sin\alpha, \\ b = P\sin\gamma - Q\cos\gamma + E\sin\theta\cos\alpha; \\ \alpha = \gamma + \varphi, \; E = zK/(y^2 - r^2), \\ z = (A^0)^{-1}(y - r). \end{cases} \tag{13}$$

The third component of the angular velocity vector can be rewritten in terms of a new variable δ as follows

$$r = r_0 + \varepsilon\delta. \tag{14}$$

We change system (7) and (12) from the variables P, Q, r, ψ, θ, φ and γ to the new ones a, b, δ, ψ, θ, α and γ in which $\alpha = \gamma + \varphi$ by using equations (13) and (14) as transformation formula from the variables P, Q and r to the variables a, b and δ. After some reductions,

we obtain the following system

$$\begin{cases}
\dot{a}=\varepsilon(A^0)^{-1}(M_1^0\cos\gamma+M_2^0\sin\gamma)-\varepsilon E(a\cos\alpha \\
\quad +b\sin\alpha)\cos\theta\sin\alpha+(A^0)^{-1}\{K-E[C(r_0+\varepsilon\delta) \\
\quad +\lambda_3]\}\sin\theta\cos\alpha+\varepsilon E\cos\theta\cos\alpha[(a\sin\alpha-b\cos\alpha) \\
\quad +E\sin\theta]+K^{-1}E\sin\theta\sin\alpha\{-\dot{K}+\varepsilon\dot{\delta}z^{-1}[2yE(C \\
\quad -A^0)(A^0)^{-1}-2E(r_0+\varepsilon\delta)-K(C-2)A^0)^{-1}]\}, \\
\dot{b}=\varepsilon(A^0)^{-1}(M_1^0\sin\gamma-M_2^0\cos\gamma)+\varepsilon E(a\cos\alpha \\
\quad +b\sin\alpha)\cos\theta\cos\alpha+(A^0)^{-1}\{K-E[C(r_0+\varepsilon\delta) \\
\quad +\lambda_3]\}\sin\theta\sin\alpha+\varepsilon E\cos\theta\sin\alpha[(a\sin\alpha-b\cos\alpha) \\
\quad +E\sin\theta]+K^{-1}E\sin\theta\cos\alpha\{\dot{K}-\varepsilon\dot{\delta}z^{-1}[2yE(C \\
\quad -A^0)(A^0)^{-1}-2E(r_0+\varepsilon\delta)-K(C-2)A^0)^{-1}]\}, \\
\dot{\delta}=\varepsilon C^{-1}M_3^0,\quad \dot{\theta}=\varepsilon(a\cos\alpha+b\sin\alpha), \\
\dot{\psi}=\varepsilon(a\sin\alpha-b\cos\alpha+E\sin\theta)\csc\theta, \\
\dot{\alpha}=(A^0)^{-1}(Cr_0+\lambda_3)+\varepsilon[C(A^0)^{-1}\delta \\
\quad -(a\sin\alpha-b\cos\alpha+E\sin\theta)\cot\theta], \\
\dot{\gamma}=n_0+(A^0)^{-1}[\lambda_3+\varepsilon(C-A^0)\delta],
\end{cases} \tag{15}$$

where

$$M_i^0(a,b,\delta,\psi,\theta,\alpha,\gamma,t)=M_i^*(P,Q,r,\psi,\theta,\varphi,t);\ i=1,2,3. \tag{16}$$

According to (13) and (14), the functions M_i^0 are periodic functions of α and γ with periods of 2π. System (15) is more convenient for further study and can be rewritten in the form

$$\begin{cases}
\dot{x}=\sum_{i=1}^{2}\varepsilon^i F_i(x,y), \\
\dot{y^1}=\omega_1+\sum_{i=1}^{2}\varepsilon^i g_i(x,y), \\
\dot{y^2}=\omega_2+\sum_{i=1}^{2}\varepsilon^i h_i(x,y); \\
\omega_1=(A^0)^{-1}(Cr_0+\lambda_3), \\
\omega_2=(A^0)^{-1}[(C-A^0)r_0+\lambda_3], \\
x(0)=x_0,\ y^1(0)=y^{10},\ y^2(0)=y^{20},
\end{cases} \tag{17}$$

where $x=(x^1,x^2,...,x^5)$ is the vector valued function and y^1, y^2 are the fast variables. The vector valued functions F_i, g_i and $h_i(i=1,2)$ can be defined from the right hand sides of (15).

We denote the two-dimensional vector $(g_1,\ h_1)$ by z_1. Hence, we assume that the perturbing moments M_i^* are independent of t.

Accordance to the procedure in [16], we will seek a change of variables of system (17) as

$$x=x^*+\sum_{i=1}^{2}\varepsilon^i u_i(x^*,y^*)+...,$$

$$y=y^*+\sum_{i=1}^{2}\varepsilon^i v_i(x^*,y^*)+...,$$

$$y=(y^1,y^2),\ \ x^*=(x^{*1},x^{*2},...,x^{*5}),$$

$$y^*=(y^{*1},y^{*2}),\ \ z_1=(g_1,h_1).$$

In terms of the new variables x^* and y^*, we can rewrite system (17) as

$$\begin{cases}
\dot{x^*}=\sum_{i=1}^{2}\varepsilon^i A_i(x^*)+..., \\
\dot{y^*}=\omega+\sum_{i=1}^{2}\varepsilon^i B_i(x^*)+...; \\
\omega=(\omega_1,\omega_2).
\end{cases} \tag{18}$$

We can choose the vector valued functions u_1, v_1 and u_2 in the following suitable forms [15]

$$\begin{cases}
\omega\frac{\partial u_1}{\partial y^*}=F_1(x^*,y^*)-A_1(x^*), \\
\omega\frac{\partial v_1}{\partial y^*}=z_1(x^*,y^*)-B_1(x^*), \\
\omega\frac{\partial u_2}{\partial y^*}=F_2(x^*,y^*)+(\frac{\partial F_1}{\partial x^*})u_1+(\frac{\partial F_1}{\partial y^*})v_1 \\
\qquad -(\frac{\partial u_1}{\partial x^*})A_1(x^*)-(\frac{\partial u_1}{\partial y^*})B_1(x^*)-A_2(x^*),
\end{cases} \tag{19}$$

where

$$\begin{cases}
A_1(x^*)=\frac{1}{4\pi^2}\int_0^{2\pi}\int_0^{2\pi}F_1(x^*,y^*)dy^{*1}dy^{*2}, \\
B_1(x^*)=\frac{1}{4\pi^2}\int_0^{2\pi}\int_0^{2\pi}z_1(x^*,y^*)dy^{*1}dy^{*2}, \\
A_2(x^*)=\frac{1}{4\pi^2}\int_0^{2\pi}\int_0^{2\pi}[F_2(x^*,y^*)+(\frac{\partial F_1}{\partial x^*})u_1 \\
\qquad +(\frac{\partial F_1}{\partial y^*})v_1-(\frac{\partial u_1}{\partial x^*})A_1(x^*) \\
\qquad -(\frac{\partial u_1}{\partial y^*})B_1(x^*)]dy^{*1}dy^{*2},
\end{cases} \tag{20}$$

and $(\frac{\partial f}{\partial x})$ will be treated as matrix of partial derivatives $\|\frac{\partial f_i}{\partial x^j}\|$ $(i,j=1,2,...,5)$. The averaged system for the slow variables up to the first and second approximations can be determined as

$$\begin{cases}
\dot{x_1^*}=\varepsilon A_1(x_1^*),\ \ \dot{x_2^*}=\sum_{i=1}^{2}\varepsilon^i A_i(x_2^*), \\
x_1^*(0)=x_{10},\ \ x_2^*(0)=x_{20}.
\end{cases} \tag{21}$$

Also, for the fast variables the system of equations in the second approximation can be obtained from

$$\dot{y_2^*} = \omega + \varepsilon B_1(x_1^*(t)),\ \ y_2^*(0) = y^0;\ \ y^0 = (y^{10}, y^{20}). \quad (22)$$

Integrating (22) to obtain

$$y_2^*(t) = y^0 + \omega t + \varepsilon \int_0^t B_1(x_1^*(s))ds. \quad (23)$$

The second system of (21) can be transformed into

$$\frac{dx_2^*}{d\tau} = A_1(x_2^*) + \varepsilon A_2(x_2^*);\ \ \tau = \varepsilon t. \quad (24)$$

Thus, the time interval $(0, \frac{\tau}{\varepsilon})$ which we considered in the original system (16) becomes $(0,T)$. The solution of system (24) can be expressed as

$$x_2^*(\tau) = x^{(1)}(\tau) + \varepsilon x^{(2)}(\tau) + O(\varepsilon^2). \quad (25)$$

Making use of (24) and (25), to obtain the following systems

$$\begin{cases} \frac{dx^{(1)}}{d\tau} = A_1(x^{(1)}), \\ \frac{dx^{(2)}}{d\tau} = A_1'(x^{(1)}(\tau))x^{(2)} + A_2(x^{(1)}(\tau)), \\ x^{(1)}(0) = x_0, \quad x^{(2)}(0) = 0. \end{cases} \quad (26)$$

where $A_1'(x) = \|\frac{\partial A_1^i}{\partial x^j}\|$ represents the matrix of partial derivatives.

Since the first system of (26) is linear, then it is easier to be investigated than system (24). So, its general solution can be expressed as

$$X'(\tau) = A_1(X), \quad X(0,c) = c = x_0.$$

Hence, the expressions for the functions $x^{(1)}(\tau)$ and $x^{(2)}(\tau)$ can be obtained in the forms

$$\begin{cases} x^{(1)}(\tau) = X(\tau, x_0), \\ x^{(2)}(\tau) = \Phi(\tau) \int_0^\tau \Phi^{-1}(\tau)\ \eta(\tau) d\tau, \end{cases} \quad (27)$$

where

$$\Phi(\tau) = \|\frac{\partial X(\tau,c)}{\partial c}\|_{c=x_0}, \quad \eta = A_2(X(\tau, x_0)).$$

Hence, the vector functions $x_\varepsilon^\nu(t)$ and $y_\varepsilon^\nu(t)$ take the forms

$$\begin{cases} x_\varepsilon^\nu(t) = x^{(1)}(\varepsilon t) + \varepsilon x^{(2)}(\varepsilon t) + \varepsilon u_1(x^{(1)}(\varepsilon t), y^0 \\ \qquad + \omega t + \varepsilon \int_0^t B_1(x^{(1)}(\varepsilon s))ds), \\ y_\varepsilon^\nu(t) = y^0 + \omega t + \varepsilon \int_0^t B_1(x^{(1)}(\varepsilon s))ds), \end{cases} \quad (28)$$

Thus, the approximate solutions $x_\varepsilon^\nu(t)$ and $y_\varepsilon^\nu(t)$ can be obtained, with the aid of Fourier series we can solve equations (19). Consequently using (20) to get the vector valued function $A_2(x^*)$. Moreover, with the aid of (27) we can determine easily from (26) the solutions $x^{(1)}(\tau)$ and $x^{(2)}(\tau)$. Then the required approximation $x_\varepsilon^\nu(t)$ and $y_\varepsilon^\nu(t)$ can be constructed directly from (28).

4 The case of dissipative moments

Now, we try to apply the averaging procedure in the previous section to obtain the approximate solutions of both the nutation and precession angles up to the first and second approximations. Taking into account relations (6) and (8); then one can write in terms of the variables $a, b, \delta, \psi, \theta, \alpha$ and γ the first three equations of system (15) in the following form, while the other equations of the same system remain unchanged

$$\begin{cases} \dot{a} = \varepsilon(A^0)^{-1}[K(R_1\sin\theta + R_2\cos\theta) + A^0 r_0(\delta_2 \\ \quad -\delta_1)R_3 + (Cr_0 - \lambda_3)(\delta_1 R_4\cos\gamma - \delta_2 R_5\sin\gamma)] \\ \quad + \sin\theta\cos\alpha(R_6 + \varepsilon^2 E^2\cos\theta) + \varepsilon E R_7\cos\theta\sin\alpha \\ \quad -EK^{-1}(\dot{K} + \varepsilon\dot{\delta}z^{-1}R_8)\sin\theta\sin\alpha, \\ \dot{b} = \varepsilon(A^0)^{-1}[-K(R_9\sin\theta + R_{10}\cos\theta) - A^0 r_0(\delta_2 \\ \quad -\delta_1)R_{11} + (Cr_0 - \lambda_3)(\delta_1 R_4\sin\gamma - \delta_2 R_5\cos\gamma)] \\ \quad + \sin\theta\sin\alpha(R_6 + \varepsilon^2 E^2\cos\theta) + \varepsilon E R_{12}\cos\theta\cos\alpha \\ \quad +EK^{-1}(\dot{K} + \varepsilon\dot{\delta}z^{-1}R_{13})\sin\theta\cos\alpha, \\ \dot{\delta} = \varepsilon KC^{-1}(y_1\sin\varphi - x_1\cos\varphi)\sin\theta. \end{cases} \quad (29)$$

where

$$\begin{cases} R_1 = (\delta_2\sin\varphi\sin\gamma - \delta_1\cos\varphi\cos\gamma), \\ R_2 = (x_1\sin\gamma - y_1\cos\gamma), \\ R_3 = [a\sin 2\gamma - b\cos 2\gamma + E\sin\theta\cos(\varphi - \gamma)], \\ R_4 = (a\sin\gamma - b\cos\gamma + E\sin\theta\cos\varphi), \\ R_5 = (a\cos\gamma + b\sin\gamma + E\sin\theta\sin\varphi), \\ R_6 = (A^0)^{-1}[K - E(C(r_0 + \varepsilon\delta) + \lambda_3)], \\ R_7 = a(\sin\alpha - \cos\alpha) - b(\sin\alpha + \cos\alpha), \\ R_8 = [2E(r_0 + \varepsilon\delta) - (A^0)^{-1}(2y(C - A^0) + K(C - 2))], \\ R_9 = (\delta_1\cos\varphi\sin\gamma + \delta_2\sin\varphi\cos\gamma), \\ R_{10} = (x_1\cos\gamma + y_1\sin\gamma), \\ R_{11} = [b\sin 2\gamma + a\cos 2\gamma + E\sin\theta\sin(\varphi - \gamma)], \\ R_{12} = a(\cos\alpha - \sin\alpha) - b(\cos\alpha + \sin\alpha), \\ R_{13} = [2E(r_0 + \varepsilon\delta) - (A^0)^{-1}(2y(C - A^0) - K(C - 2))]. \end{cases}$$

To construct the approximate solution of system (29), we apply the averaging procedure being described in the

previous section. The vector valued functions A_1, B_1 and B_2 that defined by (20) take the forms

$$\begin{cases} A_1 = \{A_1^{(i)}\},\ B_1 = \{B_1^{(j)}\};\ (i=1,2,...,5),\ (j=1,2) \\ A_1^{(1)} = -\frac{b}{2}R_{14} - \frac{1}{16}(KE)^{-1}He\ell'^2[R_{15}R_{16} - 8aE^2\sec^2\theta \\ \quad \times \tan^2\theta - bE^{-1}\sec\theta(R_{17}R_{18} - 4ba^2R_{19})], \\ A_1^{(2)} = \frac{a}{2}R_{14} + \frac{1}{32}(KE)^{-1}He\ell'^2[R_{15}R_{20} - 16bE^2\sec^2\theta \\ \quad \times \tan^2\theta - E^{-1}\sec\theta(2aR_{17}R_{19} - 4ab^2R_{18})], \\ A_1^{(3)} = 0, \quad A_1^{(4)} = E, \quad A_1^{(5)} = 0, \\ B_1^{(1)} = C(A^0)^{-1}\delta - E\cos\theta, \quad B_1^{(2)} = (C-A^0)(A^0)^{-1}\delta, \end{cases} \tag{30}$$

and

$$\begin{cases} A_2^{(1)} = \frac{b}{32}K^{-1}He\ell'^2[R_{21} - 2E^{-1}(a^2+b^2) \\ \quad \times R_{22}\csc^2\theta - E^{-2}(5a^2+b^2)R_{23}], \\ A_2^{(2)} = -\frac{a}{32}K^{-1}He\ell'^2[R_{21} - 2E^{-1}(a^2+b^2) \\ \quad \times R_{22}\csc^2\theta - E^{-2}(a^2+5b^2)R_{23}], \\ A_2^{(3)} = 0, \quad A_2^{(4)} = \frac{K\delta(C-2A^0)}{R_{24}}, \quad A_2^{(5)} = 0. \end{cases} \tag{31}$$

where

$$\begin{cases} R_{14} = (A^0)^{-1}(\delta_1+\delta_2)(Cr_0-\lambda_3) + 2E\cos\theta, \\ R_{15} = 4E^{-1}\cot\theta\csc\theta[2E^2\sin^2\theta - (a^2+b^2)], \\ R_{16} = byE(1-\sin\theta) + bK(A^0)^{-1}\sin\theta, \\ R_{17} = 3a^2+b^2-4E^2\sin^2\theta, \\ R_{18} = yE(1-\sin\theta) + K(A^0)^{-1}\sin\theta, \\ R_{19} = yE(1-\sin\theta) - K(A^0)^{-1}\sin\theta, \quad R_{20} = 2aR_{19}, \\ R_{21} = 8E^2(2+\tan^2\theta)\sin^3\theta + 4\cos\theta(\tan^2\theta - 2) \\ \quad \times(\delta + E\cos\theta), \\ R_{22} = 1 + 2(\delta E^{-1} + \cos\theta)\cos\theta - E(4+\tan^2\theta)\sin^3\theta, \\ R_{23} = (\delta + E\cos\theta)\sec\theta, \\ R_{24} = (C^2 - 2A^0)(r_0+\delta) + (1+2A^0)\lambda_3^2. \end{cases}$$

Taking into account relations (30) for the slow and fast variables, one can obtain easily the solution of the averaged system (29) in the form

$$\begin{cases} a^{(1)} = P_0\cot\eta t + Q_0\sin\eta t \\ \quad -E_0\sin\theta_0\sin\eta t + \varphi_0, \\ b^{(1)} = -P_0\cot\eta t + Q_0\sin\eta t \\ \quad +E_0\sin\theta_0\cos\eta t + \varphi_0, \\ \gamma^{(1)} = (A^0)^{-1}[(C-A^0)r_0 + \lambda_3]t, \\ \alpha^{(1)} = C(A^0)^{-1}r_0 + [(A^0)^{-1}\lambda_3 \\ \quad -E_0\cos\theta_0]t + \varphi_0, \\ \psi^{(1)} = \psi_0 + \varepsilon E_0 t, \quad \theta^{(1)} = \theta_0. \end{cases} \tag{32}$$

where

$$\begin{cases} \eta = (I_1^2 - I_2^2)^{\frac{1}{2}}; \\ I_1 = \frac{Cr_0}{2}(A^0)^{-1}(\delta_1+\delta_2) + E_0\cos\theta_0, \\ I_2 = \frac{r_0}{2}[K(A^0)^{-1} + KC^{-1} + E_0]\tan\theta_0\sin\theta_0\sin 2\varphi. \end{cases}$$

Making use of (28), (30), (31) and (32), we can construct the components of the function $x_\varepsilon^\nu(t)$ corresponding to the angles ψ and θ in the case of dissipative moments (8) in the form

$$\begin{cases} \psi_\varepsilon^\nu(t) = \psi_0 + \varepsilon[E_0 t - R_{25}\csc\theta_0] + \frac{1}{4}\varepsilon^2[E_0R_{26} \\ \quad +He\ell'^2R_{27} + E_0^2\sin 2\theta_0], \\ \theta_\varepsilon^\nu(t) = \theta_0 + \varepsilon A^0(Cr_0)^{-1}[R_{28} \\ \quad +E_0\sin\theta_0\cos(\eta t + \varphi_0 - \alpha^{(1)})]. \end{cases} \tag{33}$$

where

$$\begin{cases} R_{25} = A^0(Cr_0)^{-1}(a^{(1)}\cos\alpha^{(1)} + b^{(1)}\sin\alpha^{(1)}), \\ R_{26} = 4r_0^{-1}(A^0E_0\cos\theta_0 - \delta), \\ R_{27} = (Cr_0)^2\sin^2\theta_0 + E_0^2(1+\sin^2\theta_0), \\ R_{28} = a^0\cos(\eta t - \alpha^{(1)}) + b^0\sin(\eta t - \alpha^{(1)}). \end{cases}$$

5 Discussion of the results

This section is devoted to ascertain accuracy of the solutions being achieved. Computer codes are presented and carried out to investigate the graphical representations for these solutions. Discussion of the results is given. For

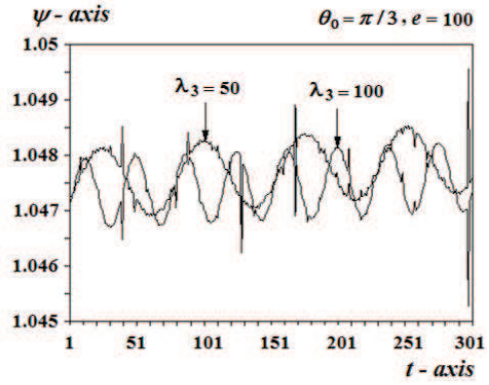

Fig. 1: Variation of the precession angle ψ via t when $\lambda_3 = 50$ and $\lambda_3 = 100$, with the same values of $\theta_0 = \pi/3$ and $e = 100$.

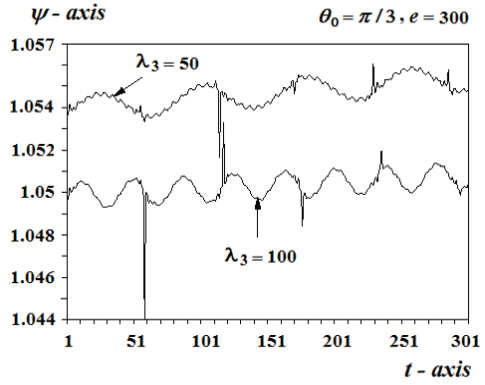

Fig. 2: Variation of the precession angle ψ via t when $\lambda_3 = 50$ and $\lambda_3 = 100$, with the same values of $\theta_0 = \pi/3$ and $e = 300$.

the mentioned problem the following data are used

$$\begin{cases} A^0 = 25kg.m^2, \ C = 17kg.m^2, \ \varepsilon = 0.001, \ M = 300kg, \\ \ell = 25m, \ T = 12.566371, \ p_0 = 0.015s^{-1}, \\ q_0 = 0.0005s^{-1}, \ e = (100, 300)coulomb, \ \ell' = 13m, \\ \delta = 7, \ \delta_1 = 50, \ \delta_2 = 40, \ \lambda_3 = (50, 100)kg.m^2.s^{-1}. \end{cases}$$

Consider ψ and θ to denote the solutions $\psi_\varepsilon^\nu(t)$ and $\theta_\varepsilon^\nu(t)$ obtained in the previous section respectively.

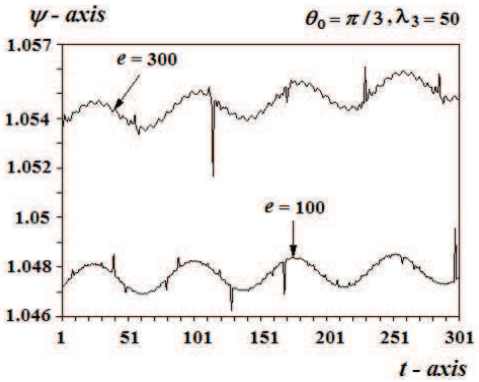

Fig. 3: The evaluation of the precession angle ψ via t when $e = 100$ and $e = 300$, with the same values of $\theta_0 = \pi/3$ and $\lambda_3 = 50$.

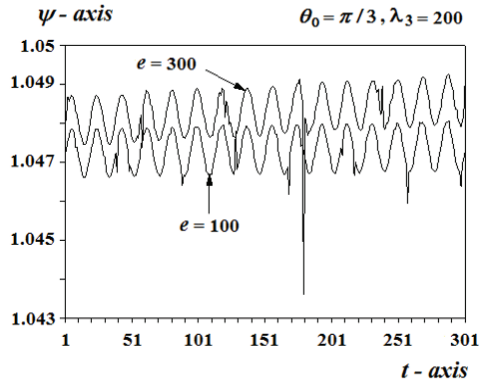

Fig. 4: The evaluation of the precession angle ψ via t when $e = 100$ and $e = 300$, with the same values of $\theta_0 = \pi/3$ and $\lambda_3 = 200$.

5.1 For the precession angle ψ

Here the concerned plots represent the functional time dependence of both the amplitudes of the waves and the oscillation frequencies revealing that (when λ_3 increases) the amplitudes of the waves decrease and the frequency numbers increase, see figures 1 and 2.
Also, when e increases, the amplitude of the waves increase and the frequency number remain unchanged, see figures 3 and 4. On other hand, when θ_0 increases the amplitude of the waves decrease and the frequency numbers remains unchanged, see figures 5 and 6. This means that the gyro oscillates about the vertical fixed axis and these oscillations decrease the amplitude of the waves without change of the frequency numbers.

5.2 For the nutation angle θ

The amplitude of the waves decreases to some extent when λ_3 increases for the same values of θ_0 and e, see figures 7 and 8. Also, we note also that, when θ_0 increases, the amplitude of the waves increases for the same values of e and λ_3, see figures 9 and 10. The change

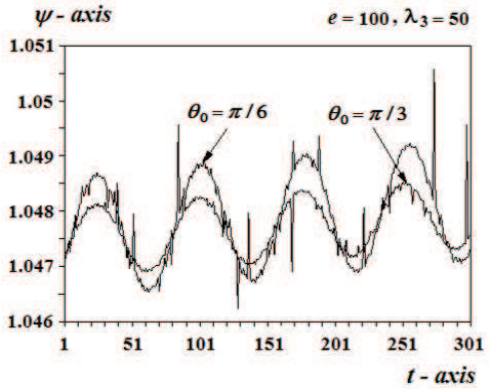

Fig. 5: The evaluation of the precession angle ψ via t when $\theta_0 = \pi/6$ and $\theta_0 = \pi/3$, with the same values of $e = 100$ and $\lambda_3 = 50$.

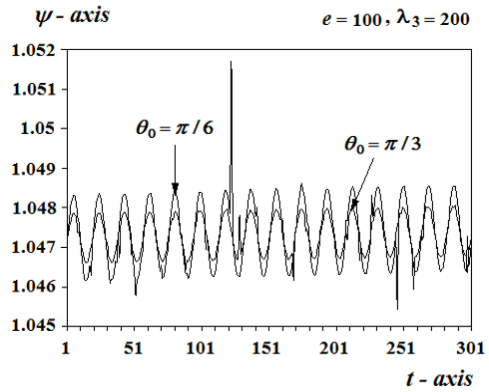

Fig. 6: Illustration of the precession angle ψ via t when $\theta_0 = \pi/6$ and $\theta_0 = \pi/3$, with the same values of $e = 100$ and $\lambda_3 = 200$.

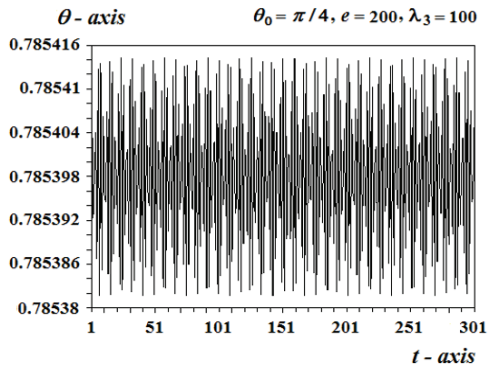

Fig. 7: Illustration of the variation of nutation angle θ via t for a nominal set of parameters $\theta_0 = \pi/4$, $e = 200$ and $\lambda_3 = 100$.

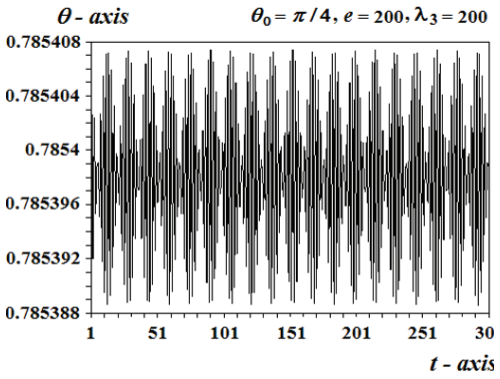

Fig. 8: Illustration of the variation of nutation angle θ via t for a nominal set of parameters $\theta_0 = \pi/4$, $e = 200$ and $\lambda_3 = 200$.

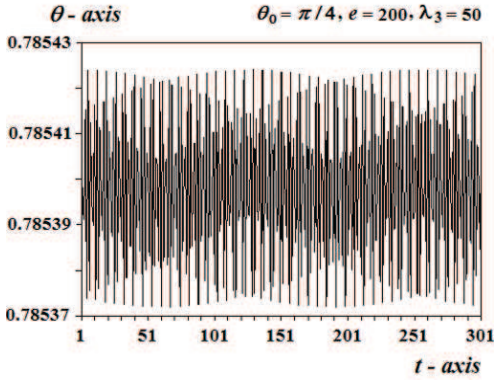

Fig. 9: Illustration of the variation of nutation angle θ via t for a nominal set of parameters $\theta_0 = \pi/4$, $e = 200$ and $\lambda_3 = 50$.

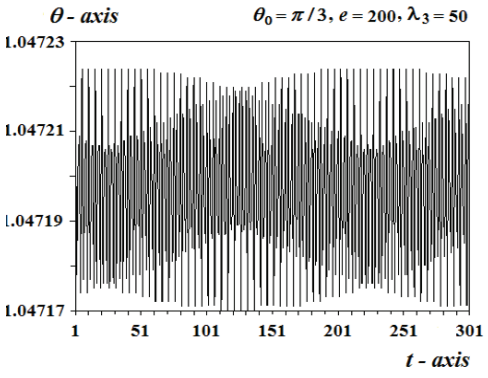

Fig. 10: Illustration of the variation of nutation angle θ via t for a nominal set of parameters $\theta_0 = \pi/3$, $e = 200$ and $\lambda_3 = 50$.

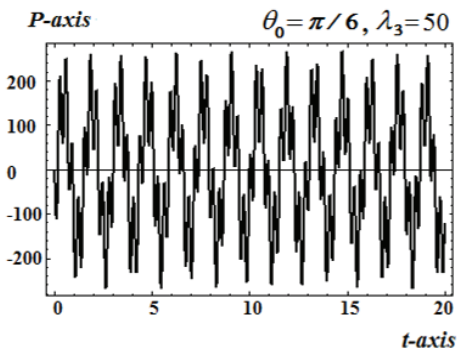

Fig. 11: Variation of the numerical solution P versus t when $\theta_0 = \pi/6$ and $\lambda_3 = 50$.

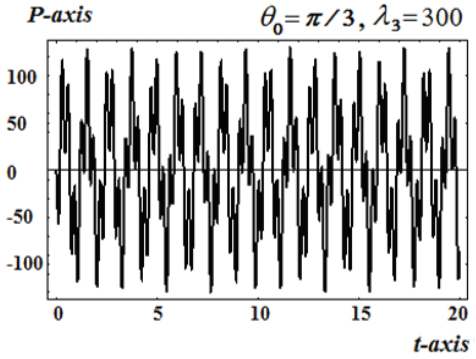

Fig. 14: Variation of the numerical solution P versus t when $\theta_0 = \pi/3$ and $\lambda_3 = 300$.

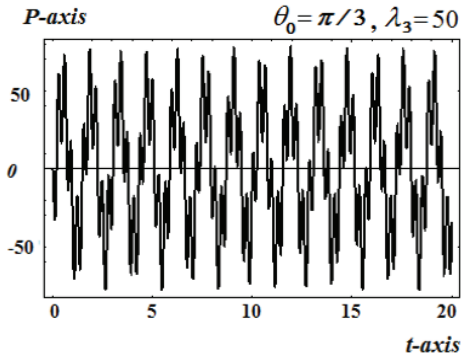

Fig. 12: Variation of the numerical solution P versus t when $\theta_0 = \pi/3$ and $\lambda_3 = 50$.

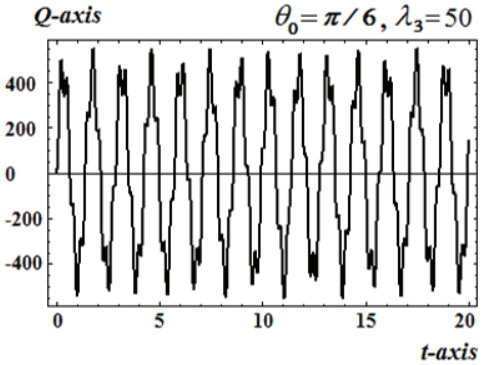

Fig. 15: Variation of the numerical solution Q versus t when $\theta_0 = \pi/6$ and $\lambda_3 = 50$.

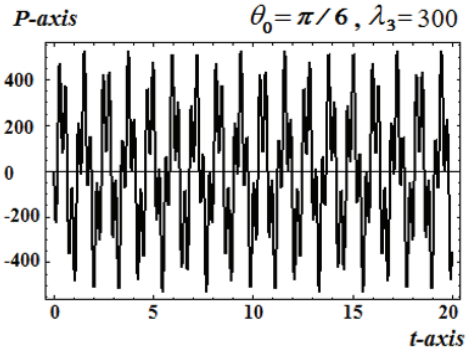

Fig. 13: Variation of the numerical solution P versus t when $\theta_0 = \pi/6$ and $\lambda_3 = 300$.

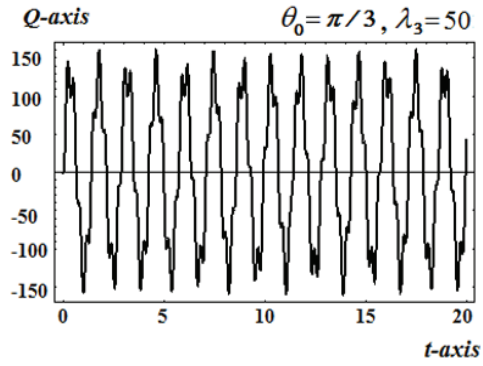

Fig. 16: Variation of the numerical solution Q versus t when $\theta_0 = \pi/3$ and $\lambda_3 = 50$.

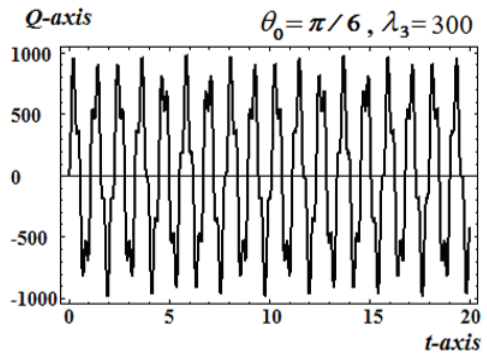

Fig. 17: Variation of the numerical solution Q versus t when $\theta_0 = \pi/6$ and $\lambda_3 = 300$.

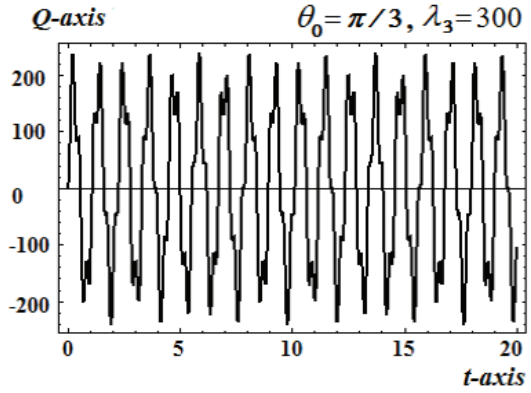

Fig. 18: Variation of the numerical solution Q versus t when $\theta_0 = \pi/3$ and $\lambda_3 = 300$.

of the nutation angle curves can be used to describe the orientation of a ship or aircraft. So, the most important practical applications of gyroscopes are met in devices for measuring the orientation or maintaining the stability of airplanes, spacecraft and submarines vehicles.

6 Numerical solutions

In this section, we are going to study the numerical solution of system (10) that consists of two second order differential equations. Taking into account the following data that be used in this system to obtain the periodic numerical solutions for each P and Q.

$$\begin{cases} \lambda_3 = (50,100)kg.m^2.s^{-1}, \;\; H = 10kg.(amper)^{-1}s^{-2}, \\ A^0 = 25kg.m^2, \;\; C = 17kg.m^2, \;\; \ell = 25m, \;\; \ell' = 13m, \\ p_0 = 0.015s^{-1}, \;\; q_0 = 0.0005s^{-1}, \;\; \theta_0 = (30^0, 60^0). \end{cases}$$

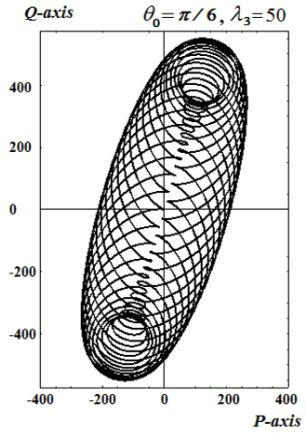

Fig. 19: The grid lines represented in the $Q-P$ plane when $\theta_0 = \pi/6$ and $\lambda_3 = 50$.

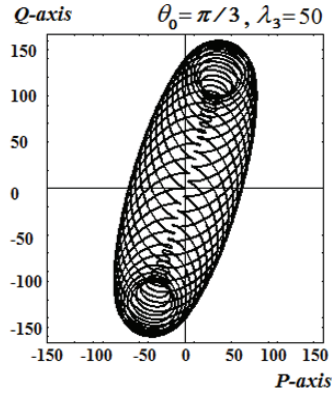

Fig. 20: The grid lines represented in the $Q-P$ plane when $\theta_0 = \pi/3$ and $\lambda_3 = 50$.

Figures (11-14) and (15-18) represent the variation of the numerical solutions for each P and Q versus time t respectively, when the initial value of the nutation angle θ_0 equals $\pi/6$ and $\pi/3$, moreover when the third component of the gyrostatic moment vector λ_3 equals $50kg.m^2.s^{-1}$ and $300kg.m^2.s^{-1}$. Also, figures (19-22) represent the variation of the numerical solutions Q against P.

In view of these plots, it is clear that when the initial value of the nutation angle increases from $\pi/6$ to $\pi/3$ for the same value of λ_3, the amplitude of the waves monotonically decreases with the stationary of frequency numbers for each P and Q, see figures (11,12) and (15,16) respectively. Consequently the grid lines density does not changed, see figures 19 and 20, while an elongation will be occurred for both P and Q axes as in figure 20 than figure 19 i.e., when θ_0 changes from $\pi/3$ to $\pi/6$.

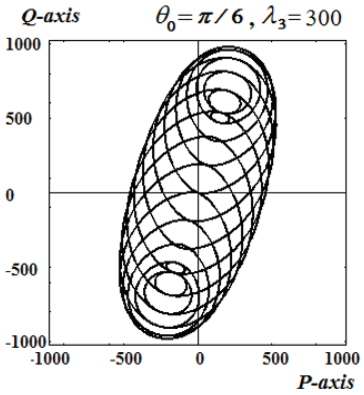

Fig. 21: The grid lines represented in the $Q-P$ plane when $\theta_0 = \pi/6$ and $\lambda_3 = 300$.

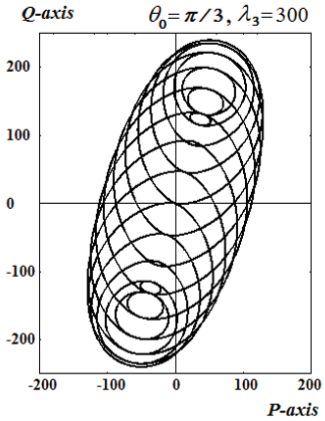

Fig. 22: The grid lines represented in the $Q-P$ plane when $\theta_0 = \pi/3$ and $\lambda_3 = 300$.

Also, when λ_3 increases from $50kg.m^2.s^{-1}$ to $300kg.m^2.s^{-1}$ for the same value of θ_0, we observe that the amplitude of the waves monotonically increases with the increase of the frequency numbers for both solutions P and Q, see figures (11,13), (12,14) and (15,17), (16,18). On the other hand, we can see that, the grid lines density decreases when λ_3 increases, see groups of figures (19, 21) and (20,12), while an elongation for each P and Q axes is observed.

From the above discussions, we can conclude that, the great effect of the third component of the gyrostatic moment vector λ_3 on the motion of the gyro with the variation of the initial value of the nutation angle. The obtained results can be used in a lot of modern industrial applications like airplanes, submarines and ships to improve any defect may be occurred.

7 Conclusion

The averaging method and its methodological treatment are presented. This method is employed to get the averaged systems of the equations of motion in both the first and second approximations. The nutation angle $\theta_\varepsilon^\nu(t)$ and precession angle $\psi_\varepsilon^\nu(t)$ are functionally dependent on the time t. They are determined up to the first and second approximations respectively and don't contain the perturbing moment parameters. The second and the third term of $\psi_\varepsilon^\nu(t)$ supplement the expression for the angular precession velocity $\omega_p = E$ and there is no dependence on the deviation of the center of gravity. The obtained solutions are considered as a generalization of previously obtained ones as Leshchenko et al. [8,33] (when $k = const$, $\lambda_3 = 0$ and in the absence of the point charge e), as Leshchenko et al. [9] (when $k = k(\theta)$, $\lambda_3 = 0$ and when the magnetic field equal to zero) and as Cid et al. [35] (when $M_i = 0$ and when the magnetic field vanishes). The numerical periodic solutions for P and Q of the system (10) are obtained and represented graphically. A great effect of the third components of the gyro moment λ_3 is shown obviously from the graphical representations.

References

[1] A. I. Ismail, T. S. Amer, Acta Mech. **154**, 31-46 (2002).
[2] A. H. Nayfeh, Perturbations methods, WILEY-VCH Verlag GmbH and Co. KGaA, Weinheim, 2004.
[3] F. A. El-Barki, A. I. Ismail, Z. Angew. Math. Mech.**75**, 821-829 (1995).
[4] T. S. Amer, Nonlinear Dyn. **54**, 249-262(2008).
[5] T. S. Amer, A. I. Ismail, W. S. Amer, J. of Aerospace Eng. **25**, 421-430 (2012).
[6] A. I. Ismail, T. S. Amer, S. A. El Banna, M. A. El-Ameen, J. Appl. Math., 1-14 (2012).
[7] L. D. Akulenko, D. D. Leshchenko, F. L. Chernousko, J. Appl. Math. Mech. **43**, 771-778 (1979).
[8] D. D. Leshchenko, A.S. Shamaev, Izv. AN SSSR MTT **22**, 8-17 (1987).
[9] D. D. Leshchenko, S. N. Sallam, J. Appl. Math. Mech. **54**, 183-190 (1990).
[10] T. S. Amer, Nonlinear Dyn. **54**, 189-198(2008).
[11] L. D. Akulenko, D. D. Leshchenko, F. L. Chernousko, Izv. AN SSSR MTT **21**, 3-10 (1986).
[12] T. A. Kozachenko, D. D. Leshchenko, MTT, Donetsk, Ukraine **39**, 62-68 (2009).
[13] A. I. Ismail, T. S. Amer, M. O. Shaker, Engng. Trans. **46**, 271-289 (1998).
[14] V. V. Sazonov, V. V. Sidorenko, J. Appl. Math. Mech. **54**, 781-787 (1990).
[15] N. N. Bogoliubov, Yu. A. Mitropolski, Asymptotic methods in the theory of non-linear oscillations, Gordon and Breach, New York, 1961.

[16] Yu. A. Mitropolski, Int. J. Non-linear Mech. **2**, 69-96 (1967).
[17] L. D. Akulenko, T. A. Kozochenko, D. D. Leshchenko, MTT **32**, 77-84 (2002).
[18] H. C. Simpson, M. D. Gunzburger, ZAMP **37**, 867-894 (1986).
[19] H. C. Simpson, M. D. Gunzburger, ZAMP **37**, 867-894 (1986).
[20] V. S. Aslanov, Spatial motion of the body during the descent in the atmosphere, Fizmatlit, Moscow, 2004.
[21] V. S. Aslanov, J. Appl. Math. Mech. **73**, 179-187 (2009).
[22] V. S. Aslanov, A. S. Ledkov, Aerosp Sci Technol. **13**, 224-231 (2009).
[23] V. S. Aslanov, A. V. Doroshin, J. Appl. Math. Mech. **74**, 524-535 (2010).
[24] A. V. Doroshin, Commun. Nonlinear Sci. Numer. Simul. **17**, 1460-1474 (2012).
[25] V. S. Aslanov, A. V. Doroshin, Mech. Solids **41**, 29-39 (2006).
[26] A. V. Doroshin, J. Appl. Math. Mech. **72**, 269-279 (2008).
[27] A. V. Doroshin, Int. J. Non-Linear Mech. **45**, 193-205 (2010).
[28] A. V. Doroshin, WSEAS Trans. Syst. Control **3**, 50-61 (2008).
[29] M. Rotea, Dyn. Control **8**, 55-80 (1998).
[30] A. I. El-Gohary, J. Appl. Math. and Comput. **151**, 163-179 (2004).
[31] A. I. El-Gohary, Chaos Soliton and Fract. **42**, 2842-2851 (2009).
[32] A. I. El-Gohary, T. S. Tawfik, Mech Res. Commun. **37**, 354-359 (2010).
[33] D. D. Leshchenko, Int. Appl. Mech. **35**, 93-99 (1999).
[34] H. William, B. John, Engineering electromagnetic, McGraw-Hill Science, 2011.
[35] R. Cid, A. Vigueras, Rev. Acad. Ciencias. Zaragoza **45**, 83-93 (1990).

T. S. Amer received his PhD degree in Applied Mathematics at Tanta University, Egypt and Magdeburg University, Germany. He works as an Associate Prof. of applied mathematics in Mathematics department. His main research interests are in the areas of applied mathematics, rigid body, gyroscopic motion, pendulum motion, perturbation and chaos. He has published research articles in reputed international journals of mathematical and engineering sciences. He is referee of international mathematical journals.